THE JOURNAL OF BIOLOGICAL CHEMISTRY VOL. 291, NO. 23, pp. 12126–12135, June 3, 2016

MicroRNA-127 Promotes Mesendoderm Differentiation of Mouse Embryonic Stem Cells by Targeting Left-Right Determination Factor 2*

Received for publication, February 23, 2016, and in revised form, April 11, 2016 Published, JBC Papers in Press, April 12, 2016, DOI 10.1074/jbc.M116.723247

Haixia Ma[‡§1], **Yu Lin**[¶1], **Zhen-Ao Zhao**[‡], **Xukun Lu**[‡], **Yang Yu**[‡], **Xiaoxin Zhang**[‡], **Qiang Wang**[¶2], **and Lei Li**[‡§3]

From the [‡]*State Key Laboratory of Stem Cell and Reproductive Biology and* [¶]*State Key Laboratory of Membrane Biology, Institute of Zoology, Chinese Academy of Sciences, 100101 Beijing and the* [§]*Institute of Zoology, University of Chinese Academy of Sciences, Beijing 100049, China*

Specification of the three germ layers is a fundamental process and is essential for the establishment of organ rudiments. Multiple genetic and epigenetic factors regulate this dynamic process; however, the function of specific microRNAs in germ layer differentiation remains unknown. In this study, we established that microRNA-127 (miR-127) is related to germ layer specification via microRNA array analysis of isolated three germ layers of E7.5 mouse embryos and was verified through differentiation of mouse embryonic stem cells. miR-127 is highly expressed in endoderm and primitive streak. Overexpression of miR-127 increases and inhibition of miR-127 decreases the expression of mesendoderm markers. We further show that miR-127 promotes mesendoderm differentiation through the nodal pathway, a determinative signaling pathway in early embryogenesis. Using luciferase reporter assay, left-right determination factor 2 (*Lefty2*), an antagonist of nodal, is identified to be a novel target of miR-127. Furthermore, the role of miR-127 in mesendoderm differentiation is attenuated by *Lefty2* overexpression. Altogether, our results indicate that miR-127 accelerates mesendoderm differentiation of mouse embryonic stem cells through nodal signaling by targeting *Lefty2*.

The specification and patterning of three germ layers are crucial processes during early development of the mouse (1). The primitive streak (PS),[4] through which epiblast cells move and form mesoderm and definitive endoderm, is a critical structure for specification of the three germ layers (2). The nodal signaling pathway plays a central role in germ layer specification and PS formation (2, 3). In this pathway, Nodal, a transforming growth factor-β (TGF-β) superfamily protein, initially interacts with and activates activin-like receptors that are serine/threonine kinases. Then, the activated activin-like receptor phosphorylates Smad2, which forms a co-Smad complex with Smad4 and is transported to the nuclei to regulate expression of target genes, eventually promoting PS formation (4–7). Lefty2 is an antagonist of the nodal pathway by competitive binding to the activin-like receptors (8). In mice, Lefty2 expresses in the anterior half of the primitive streak and the left part of the lateral plate mesoderm of the gastrulating embryo (9, 10). *Lefty2* mutant mouse embryos form enlarged PS and immoderate mesoderm (11). Thus, Lefty2 is required for the formation of PS, and its expression is precisely controlled during mouse gastrulation. However, an understanding of the mechanism of *Lefty2* regulation during this process remains elusive.

MicroRNAs (miRNAs) are 19–25-nucleotide single strand RNAs that are widespread in organisms and play important roles in diverse biological processes, including animal development, by controlling the expression of related genes (12, 13). Mature miRNAs are generated from endogenous transcripts with a hairpin-shaped structure that functions as a complex known as the RNA-induced silencing complex, which inhibits protein translation and destabilizes mRNA transcripts (12, 13). RNase III family member DICER and double strand RNA-binding protein DiGeorge syndrome critical region gene 8 (Dgcr8) play crucial roles in the production of mature miRNAs (12, 14). Knock-out of *Dicer* impairs the generation of both endo-siRNAs and miRNAs. The embryonic region of the E7.5 *Dicer* mutant embryo is obviously small and malformed, with decreased *Oct4* expression (15). In addition, the differentiation potential of *Dicer*-deficient embryonic stem cells (ESCs) is severely destructed *in vitro* and *in vivo* (16, 17). Similarly, knock-out of *Dgcr8* results in embryonic lethality at E6.5, and *Dgcr8* knock-out ESCs cannot form the cystic embryoid bodies (EBs) that consist of a group of cells representing the three germ layers of the early mouse embryo (18). Thus, miRNAs are critical for mouse early embryonic development and may play roles in germ layer specification.

miR-127 is located on mouse distal chromosome 12 and on human chromosome region 14q32, which are well known as a *Dlk1/Gtl2* imprinted region. miR-127 lies near a CpG island in *Rtl1*, a paternally expressed gene, and takes an antisense strand of *Rtl1* as a template for transcription but is expressed from the maternal chromosome (19). Mice with disrupted miR-127 have placental defects in the labyrinthine zone (20). In addition, overexpression of miR-127 affects

* This work was supported by National Natural Science Foundation of China Grants 31590832 and 31471353, National Basic Research Program of China Grant 2012CB944401, and Strategic Priority Research Program of the Chinese Academy of Sciences Grant XDA01010103. The authors declare that they have no conflicts of interest with the contents of this article.

[1] Both authors contributed equally to this work.
[2] To whom correspondence may be addressed. Tel.: 86-10-64807895; Fax: 86-10-64807895; E-mail: qiangwang@ioz.ac.cn.
[3] To whom correspondence may be addressed. Tel.: 86-10-64807865; Fax: 86-10-64807865; E-mail: lil@ioz.ac.cn.

[4] The abbreviations used are: PS, primitive streak; miR-127, microRNA-127; *Lefty2*, left-right determination factor 2; ESC, embryonic stem cell; EB, embryoid body; EpiSC, epiblast stem cell; qRT, quantitative RT; ANOVA, analysis of variance; miRNA, microRNA.

lung development in the fetal lung organ culture system (21). However, the role of miR-127 is still unclear during gastrulation of mouse early development.

In this study, we explored the relationship between miR-127 and mouse germ layer differentiation during gastrulation, using microRNA array analysis of germ layers of E7.5 embryos. We found that miR-127 was enriched in endoderm and primitive streak of E7.5 mouse embryos. Overexpression of miR-127 accelerates, whereas miR-127 knockdown impedes, mesendoderm differentiation. Furthermore, we showed that miR-127 directly down-regulated the expression of *Lefty2*, an antagonist of nodal signaling and a regulator of PS formation. Thus, our results suggested that miR-127 promotes mesendoderm differentiation by down-regulating the expression of *Lefty2*.

Experimental Procedures

Mouse Maintenance, E7.5 Mouse Embryo Germ Layer Separation and Microarray—Mice were maintained under specific pathogen-free conditions (12 h of light and 12 h of dark) in the animal facilities of the Institute of Zoology. All animal experiments were performed in accordance with the guidelines of the Animal Care and Use Committee of the Institute of Zoology at the Chinese Academy of Sciences.

E7.5 embryos were dissected from 30 pregnant ICR mice and stored in a 25 mM HEPES-buffered DMEM solution containing 10% FBS. The Reichert's membrane was removed. The embryonic region was separated using a needle, rinsed in serum-free medium, incubated in pancreatic enzyme solution at 4 °C for 10 min, and transferred into HEPES-buffered DMEM solution. The embryo was then gently sucked into a siliconized Pasteur pipette to remove the endoderm layer. Needle points were inserted under the mesoderm, and each mesoderm wing was cut off. The remainder was collected as ectoderm. Total RNA was extracted with mirVana™ miRNA isolation kit (Ambion) and sent to the Bioassay Laboratory of CapitalBio Corp. for microarray and analysis.

Embryonic Stem Cell Culture, Transfection and EB Differentiation—Mouse ESCs (CMTI-1, Millipore) were maintained on mouse embryonic fibroblasts treated by mitomycin C in DMEM containing 15% fetal bovine serum, 2 mM sodium pyruvate, 2 mM L-glutamine, 0.1 mM nonessential amino acids, 50 μg/ml penicillin/streptomycin, 0.1 mM β-mercaptoethanol, and 10 ng/ml leukemia inhibitory factor. The ESCs were cultured on gelatin-coated plates in N2B27 medium before transfection, as described previously (22). Mouse ESCs were plated in 12-well plates (1×10^5 cells/well) at the time of transfection. The miRNA mimics or inhibitors (Invitrogen) were transfected with the indicated concentrations into ESCs using Lipofectamine 2000 reagent (Invitrogen). For EB formation, ESCs were trypsinized into single cells and cultured by seeding 1,000 ESCs in 30-μl hanging droplets of ES medium devoid of leukemia inhibitory factor.

RNA Isolation, Reverse Transcription, and Quantitative Real Time PCR—Total RNA was extracted with RNAzol (Molecular Research Center). Synthesis of cDNA was performed with SYBR PrimeScript™ miRNA RT-PCR kit (Takara) and PrimeScript™ RT-PCR kit (Takara), respectively, for miRNA and mRNA analyses. Real time PCR was carried out in the LightCycler 480 II system (Roche Applied Science). The primer sequences are listed in Table 1. *Hprt* and *U6* were used as reference genes for normalization of mRNA and miRNA levels. Data were processed using the 2[caret]−ΔΔ*Ct* method.

TABLE 1
Primers for qRT-PCR

Gene		Sequence (5′–3′)
miR-127	Forward	TCGGATCCGTCTGAGCTTGGCT
U6	Forward	CTCGCTTCGGCAGCACA
	Reverse	AACGCTTCACGAATTTGCGT
Sox17	Forward	CTTTATGGTGTGGGCCAAAG
	Reverse	TTCCAAGACTTGCCTAGCATC
Foxa2	Forward	CCATCAGCCCCACAAAATG
	Reverse	CCAAGCTGCCTGGCATG
Foxf1	Forward	GCATCCCTCGGTATCACTCAC
	Reverse	ATCCTCCGCCTGTTGTATGC
T	Forward	CCTCCATGTGCTGAGACTTG
	Reverse	TCACAAAAAACTGGACCACA
Flk-1	Forward	GCCCTGCTGTGGTCTCACTAC
	Reverse	CAAAGCATTGCCCATTCGAT
Gsc	Forward	ACCATCTTCACCGATGAGCAGC
	Reverse	CTTGGCTCGGCGGTTCTTAAAC
Pax6	Forward	TAACGGAGAAGACTCGGATGAAGC
	Reverse	CGGGCAAACACATCTGGATAATGG
Otx2	Forward	CAGCGTCCATCTCCCCAC
	Reverse	GTTGAGCCAGCATAGCCTTG
Sox2	Forward	GGCAGCTACAGCATGATGCAGGAGC
	Reverse	CTGGTCATGGAGTTGTACTGCAGG
Fgf5	Forward	GAAATATTTGCTGTGTCTCAGGG
	Reverse	TAAATTTGGCACTTGCATGG
Hprt	Forward	GCCAGTAAAATTAGCAGGTGTTCT
	Reverse	ATAGGCTCATAGTGCAAATCAAAAG

Luciferase Reporter Assay—The 3′UTR sequences of *Lefty2*, *Fstl3*, *Smad7*, and *Ppm1b*, including the predicted miRNA-binding site, and 3′UTR of *Lefty2* with site-directed mutagenesis were amplified from mouse ESC cDNA and then inserted into pGL3-control vector (Promega). HEK293FT cells were grown in DMEM with 10% FBS and seeded in 24-well plates before transfection with Lipofectamine 2000 (Invitrogen). The cells were co-transfected with 500 ng of firefly luciferase reporter vector pGL3 containing 3′UTR and 20 ng of *Renilla* luciferase vector pRL-TK, which was used to normalize luciferase activity. miR-127 mimics at a concentration of 20 μM or scrambled oligonucleotides were added into each well. Luciferase reporter assay was conducted 48 h after transfection using the Dual-Luciferase® reporter assay kit (Promega).

Western Blot Analysis—Whole-cell lysates were prepared by resuspending cells in RIPA lysis buffer, which contained 1% Triton X-100, 50 mM Tris-HCl (pH 7.5), 150 mM NaCl, 1% sodium deoxycholate, 0.1% SDS, 5 mM EDTA, 1 mM Na_3VO_4, and 5 mM NaF. Proteins were separated with SDS-PAGE and subsequently to Western blot (Bio-Rad). Western blot analysis was conducted with antibodies as follows: rabbit anti-Foxa2 (1:1,000, catalog no. 8186, Cell Signaling Technology); goat anti-T (1:1,000, catalog no. sc-17745, Santa Cruz Biotechnology); mouse anti-Gapdh (1:1,000, catalog no. DKM9002, Sungene); rabbit anti-phosphor (Ser-465/467)-Smad2 (1:1,000, catalog no. 3108, Cell Signaling Technology); rabbit anti-Smad2 (1:1,000, catalog no. 5339, Cell Signaling Technology); mouse anti-actin (1:1,000, catalog no. 214673, Cell Signaling Technology); rabbit anti-β-catenin (1:1,000, catalog no. 8814S, Cell Signaling Technology); and rabbit anti-Lefty2 (1:500, 13991-1-AP, Proteintech).

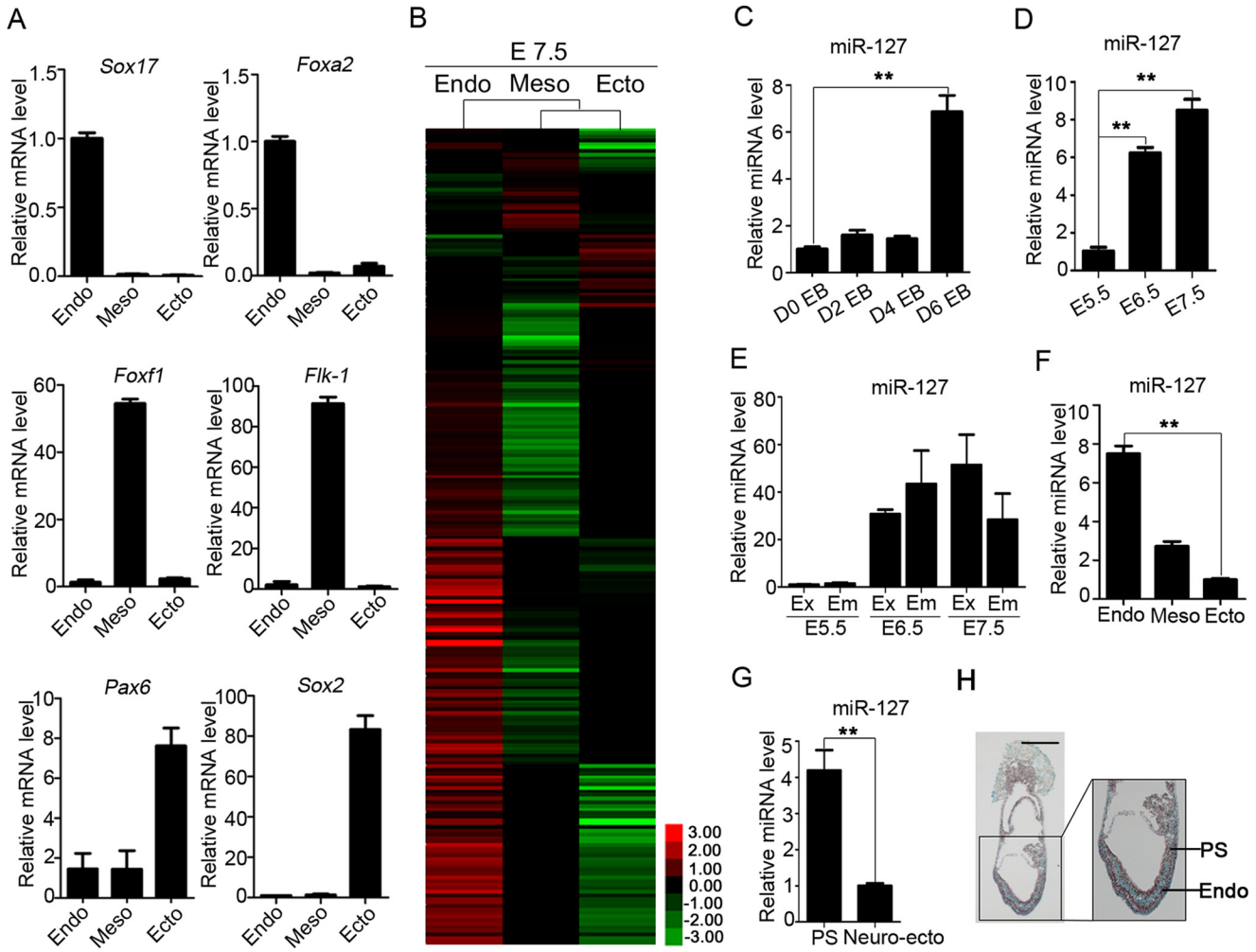

FIGURE 1. **miR-127 is associated with germ layer formation and is mainly expressed in PS and endoderm of E7.5 mouse embryo.** *A,* qRT-PCR shows lineage marker expression in detached germ layers of E7.5 embryos. *B,* heat map was generated by performing miRNAs specifically expressed in endoderm (*Endo*), mesoderm (*Meso*), and ectoderm (*Ecto*) of E7.5 mouse embryos, respectively. *C,* qRT-PCR shows miR-127 expression during EB formation (one-way ANOVA, **, $p < 0.01$). *D,* qRT-PCR shows miR-127 expression in gastrulating embryos from E5.5 to E7.5 (one-way ANOVA, **, $p < 0.01$). *E,* qRT-PCR shows miR-127 expression pattern in extra-embryonic field and embryonic region of E5.5, E6.5, and E7.5 embryos. *F,* qRT-PCR shows miR-127 expression in germ layers of E7.5 mouse embryos (one-way ANOVA, **, $p < 0.01$). *G,* qRT-PCR shows miR-127 expression in PS and neuro-ectoderm (one-way ANOVA, **, $p < 0.01$). *H,* expression of miR-127 in E7.5 embryo, shown by *in situ* hybridization. *Brown* represents miR-127 expression. *Scale bar,* 300 μm.

miRNA Oligonucleotide Injection and Whole-mount in Situ Hybridization in Zebrafish Embryos—Zebrafish embryos used in this study were derived from Tuebingen strain and raised in Holtfreter's solution at 28.5 °C. miR-127 mimics were injected into one-cell stage zebrafish embryos. After 6 h, these embryos were collected. Whole-mount *in situ* hybridization was performed according to standard procedures with probes, including *chordin*, *goosecoid,* and *lefty2* (23).

Statistical Analyses—Quantitative analyses were performed in at least three independent biological samples. Data were expressed as the means ± S.E. Statistics were conducted by using SPSS 18.0, and data were subjected to Student's *t* test or one-way analysis of variance (ANOVA). $p < 0.05$ was considered as significant.

Results

miR-127 Is Associated with Mouse Germ Layer Specification—To identify the miRNAs involved in germ layer differentiation, miRNA microarray profiling was conducted using isolated endoderm, mesoderm, and ectoderm from the embryonic region of E7.5 ICR mouse embryos. Quantitative RT-PCR (qRT-PCR) showed that the markers of each germ layer were specifically expressed in the separated sample counterparts (Fig. 1*A*), indicating effective separation and minimal contamination of each germ layer sample. miRNA microarray profiling of the three germ layers was then performed, and the miRNAs expressed in each germ layer were clustered (Fig. 1*B*). Our results showed that most miRNAs are highly enriched in endoderm. Using a criterion of an expression fold change of >3, we screened out 30 miRNAs with comparatively high expression in endoderm.

To investigate the specific miRNAs involved in germ layer differentiation, we examined the expression of 30 miRNAs at days 0, 2, 4, and 6 during EB formation, a model of ESC differentiation into germ layer lineages. Although expression of most miRNAs was unaltered, expression of miR-127 was significantly up-regulated during EB differentiation (Fig. 1*C*). These results indicated that miR-127 is likely associated with germ layer differentiation.

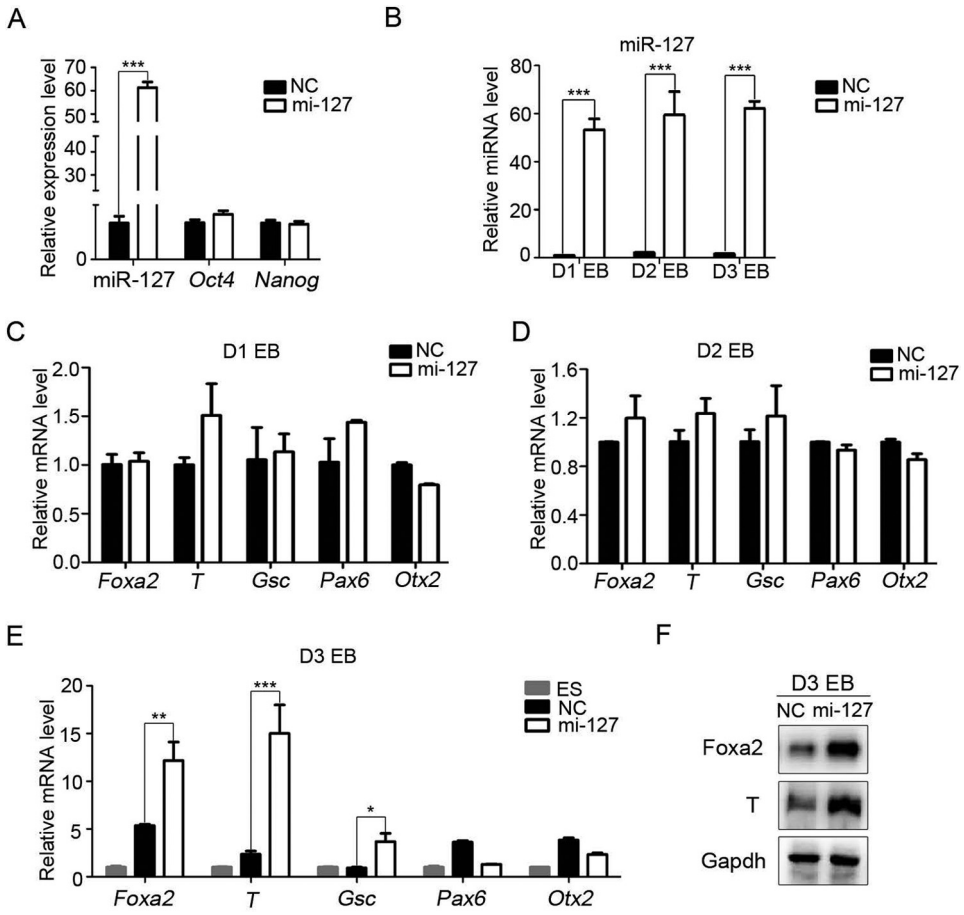

FIGURE 2. **Overexpression of miR-127 promotes mesendoderm differentiation.** *A,* qRT-PCR displays the expression of miR-127 and pluripotent markers in miR-127-overexpressed ESCs. The significance of expression was analyzed by Student's *t* test, and data are presented as means ± S.E. ($n = 3$, ***, $p < 0.001$). *B,* qRT-PCR displays the expression of miR-127 in miR-127-overexpressed days 1–3 EBs. The data are presented as means ± S.E. ($n = 3$). *C,* qRT-PCR displays lineage markers expression in miR-127-overexpressed day 1 EBs. The data are presented as means ± S.E. ($n = 3$). *D,* qRT-PCR displays lineage marker expression in miR-127-overexpressed day 2 EBs. The data are presented as means ± S.E. ($n = 3$). *E,* qRT-PCR displays lineage marker expression in miR-127-overexpressed day 3 EBs. Significant differences in expression between the designated pairs were analyzed by Student's *t* test with equal variance, and the data are presented as means ± S.E. ($n = 3$, *, $p < 0.05$; **, $p < 0.01$; ***, $p < 0.001$). *F,* Western blot shows mesendoderm marker expression in miR-127-overexpressed day 3 EBs. Gapdh was served as a loading control.

miR-127 Is Highly Expressed in Endoderm and Primitive Streak in E7.5 Embryos—We then measured miR-127 expression during mouse embryonic development using qRT-PCR. The expression of miR-127 was up-regulated progressively in E5.5 to E7.5 embryos (Fig. 1*D*) with expression in both the embryonic region and extra-embryonic tissue (Fig. 1*E*). Of the three germ layers of the E7.5 embryo, miR-127 was enriched in the endoderm, cells of which were partially derived from PS (Fig. 1*F*). To further investigate the expression of miR-127 in the E7.5 embryo, PS and neuro-ectoderm were isolated by micro-dissection. miR-127 was highly expressed in PS (Fig. 1*G*). The results from *in situ* hybridization showed a relatively high expression level of miR-127 in endoderm and PS in E7.5 embryo (Fig. 1*H*).

miR-127 Promotes Mesendoderm Differentiation—To explore the function of miR-127, we transfected miR-127 mimics to mouse ESCs to exogenously overexpress miR-127. The expression level of miR-127 increased ~60-fold in ESCs transfected with mimics, and miR-127 overexpression did not affect the pluripotency of ESCs examined by the expressions of *Oct4* and *Nanog* (Fig. 2*A*). Furthermore, the overexpression of miR-127 was consistently observed in EBs on days 1–3 during ESC differentiation (Fig. 2*B*). Next, we detected lineage marker expression after spontaneous differentiation of ESCs into EBs. Compared with controls, expression of germ layer markers did not change on day 1 and 2 EBs (Fig. 2, *C* and *D*); however, mesendoderm markers *Foxa2*, *Brachyury* (*T*), and *Gsc* were significantly up-regulated on day 3 EBs when miR-127 was overexpressed, with almost unchanged expression of ectoderm markers (*Pax6* and *Otx2*; Fig. 2*E*). At the protein level, mesendoderm markers (Foxa2 and T) were also increased on day 3 EBs with miR-127 overexpression (Fig. 2*F*). These data suggested that miR-127 promotes mesendoderm differentiation.

We then performed a loss-of-function study *in vitro* by transfecting miR-127 inhibitors (Si-127) into ESCs. miR-127 expression was reduced by ~90% in Si-127-transfected ESCs, and the pluripotent markers remained unaltered (Fig. 3*A*). The expression of miR-127 was consistently decreased during ESC differentiation (Fig. 3*B*). Next, miR-127 knockdown ESCs were differentiated to EBs, and germ layer marker expression was measured. Compared with the control, miR-127 knockdown did not affect lineage marker expression on day 3 EBs (Fig. 3*C*). We speculated that the originally low expression of miR-127 during the early stages of ES differentiation (Fig. 1*C*) results

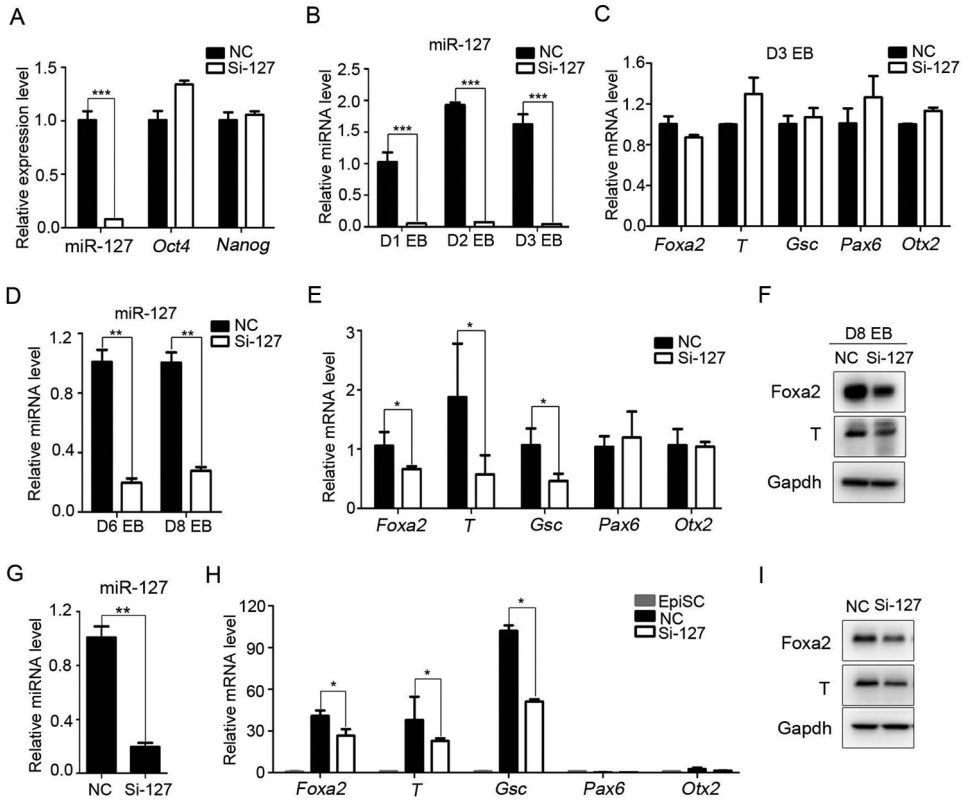

FIGURE 3. **miR-127 knockdown inhibits mesendoderm differentiation.** *A,* qRT-PCR shows expression of miR-127 and pluripotent markers in miR-127 knockdown ESCs. The significance of expression was analyzed by Student's *t* test, and data are presented as means ± S.E. ($n = 3$, ***, $p < 0.001$). *B,* qRT-PCR displays the expression of miR-127 in miR-127 knockdown days 1–3 EBs. The data are presented as means ± S.E. ($n = 3$). *C,* qRT-PCR displays lineage marker expression in miR-127 knockdown day 3 EBs. The data are presented as means ± S.E. ($n = 3$). *D,* qRT-PCR displays the expression of miR-127 on day 6 and 8 EBs following miR-127 knockdown on day 6 EBs. The data are presented as means ± S.E. ($n = 3$). *E,* qRT-PCR shows miR-127 expression on day 6 knockdown EBs and lineage marker expression on day 8 EBs following miR-127 knocked down on day 6 EBs. The significance of expression was analyzed by Student's *t* test, and data are presented as means ± S.E. ($n = 3$, *, $p < 0.05$). *F,* expression of mesendoderm markers in negative control (*NC*) and miR-127 knockdown day 8 EBs (negative control and Si-127), revealed by Western blot. Gapdh served as loading control. *G,* qRT-PCR shows miR-127 expression in miR-127 knockdown EpiSC cells. The significance of expression was analyzed by Student's *t* test, and data are presented as means ± S.E. ($n = 3$, **, $p < 0.01$). *H,* qRT-PCR shows lineage marker expression in EpiSC cells treated with 10 ng/ml activin A followed by control and miR-127 inhibitor transfected (negative control and Si-127). The significance of expression was analyzed using Student's *t* test, and data are presented as means ± S.E. ($n = 3$, *, $p < 0.05$). *I,* expression of mesendoderm markers (Foxa2 and T) was analyzed by Western blot. Gapdh was used as a loading control.

in no effect of miR-127 knockdown in this system. As miR-127 peaked on day 6 EBs, we attempted to knock down miR-127 expression on day 6 EBs, and we examined the expression of germ layer markers 2 days later. The expression of miR-127 was decreased by ~70% (Fig. 3*D*), and mRNA of mesendoderm markers (*Foxa2*, *T* and *Gsc*) was significantly down-regulated in Si-127-transfected cells (Fig. 3*E*). Furthermore, Foxa2 and T protein were decreased in Si-127-transfected cells (Fig. 3*F*). The expression of ectoderm markers (*Pax6* and *Otx2*) remained unaltered in the miR-127 knockdown cells (Fig. 3*E*).

To confirm the role of miR-127 in mesendoderm differentiation, we transfected miR-127 inhibitor into epiblast stem cells (EpiSCs) and induced these cells to differentiation using activin A. After the miR-127 inhibitor treatment, miR-127 expression decreased by ~80% in EpiSCs (Fig. 3*G*). Consistently, miR-127 knockdown decreased mesendoderm marker expression at RNA (*Foxa2*, *T*, and *Gsc*) and protein (Foxa2 and T) levels during the differentiation of miR-127 knockdown EpiSCs (Fig. 3, *H* and *I*). Collectively, these data implied that miR-127 specifically promotes mesendoderm differentiation.

miR-127 Functions by Nodal Pathway—To unravel how miR-127 functions in mesendoderm differentiation, we carried out functional cluster analysis of the potential targets of miR-127 predicted from miRBase. We found that these miR-127 targets were mainly clustered in two developmental pathways, including nodal and Wnt signaling. We showed that miR-127 overexpression promoted mesendoderm marker expression on day 3 EBs (Fig. 2, *E* and *F*). Then, we examined the expression of key effectors (active β-catenin and phosphorylated Smad2) of these pathways in control and miR-127-overexpressed EBs at day 2. Overexpression of miR-127 increased phosphorylated Smad2 (p-Smad2) but not active β-catenin (Fig. 4, *A* and *B*). These data suggested miR-127 may be involved in the nodal pathway.

To investigate the pathways mediated by miR-127 in mesendoderm differentiation, we induced mouse ESC differentiation to mesendoderm with activin A. We treated ESCs with 10 ng/ml activin A after 1 day of culture in leukemia inhibitory factor-free medium (24, 25). When ESCs were treated for 48 h, mesendoderm markers (Foxa2 and T) were up-regulated, indicating ESCs were successfully induced into mesendoderm (Fig. 4, *C* and *D*). We also examined the expression of miR-127 in this differentiation system. Our results showed that miR-127 was up-regulated accompanying the increased expression of mesendoderm markers (Fig. 4*D*).

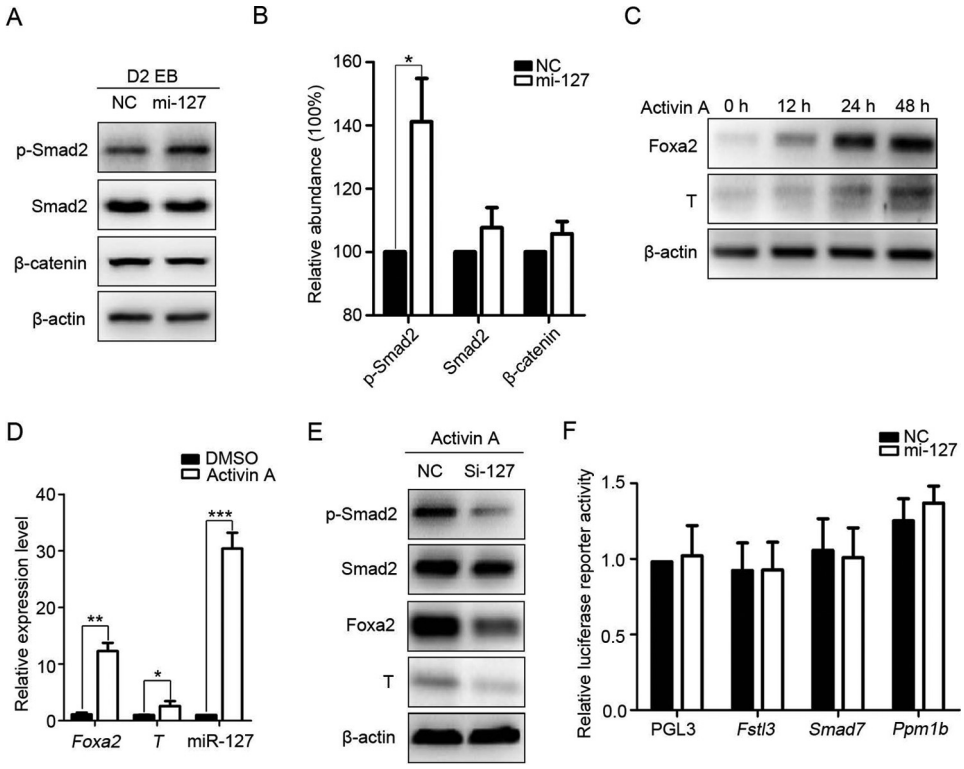

FIGURE 4. **miR-127 involved in nodal signaling pathway.** *A,* effectors of nodal and Wnt pathway expression were measured on day 2 EBs by Western blot. GAPDH was used as loading control. *B,* analysis of gray scale scanning of Western blot results of signaling effectors on day 2 EBs. The data were from three independent experiments (*, $p < 0.05$). *C,* mesendoderm marker expression in ESCs treated with activin A for 0, 12, 24, and 48 h, displayed by Western blot. *D,* qRT-PCR shows *Foxa2*, *T*, and miR-127 expression in ESCs treated with 10 ng/ml activin A. The significance of expression was analyzed by Student's *t* test, and data are presented as means ± S.E. ($n = 3$, *, $p < 0.05$; **, $p < 0.01$; ***, $p < 0.001$). *E,* expression of p-Smad2 and mesendoderm markers in miR-127 knockdown ESCs under activin A treatment, shown by Western blot. *β*-actin was used as loading control. *F,* luciferase report vectors containing the binding site of miR-127 in 3′UTR and either miR-127 mimics or negative control (*NC*), co-transfected into 293FT cells, with relative luciferase activity measured. PGL3 vector acted as a control. *NC*, negative control.

We then knocked down miR-127 when ESCs differentiated to mesendoderm. Upon activin A stimulation, both p-Smad2 and mesendoderm markers (Foxa2 and T) were down-regulated in miR-127 knockdown cells compared with the control (Fig. 4*E*). These findings suggested that miR-127 accelerates mesendoderm differentiation through activin/nodal signaling.

miR-127 Is Involved in the Nodal Pathway through Lefty2 during Mesendoderm Differentiation—As miR-127 promotes mesendoderm differentiation through the activin/nodal signaling pathway, we focused on the targets annotated to be associated with this pathway from the miRBase to identify the specific targets of miR-127. Among 15 predicted targets, four genes (*Lefty2*, *Fstl3*, *Smad7*, and *Ppm1b*) were reported to negatively regulate nodal signaling (11, 26–28), reminiscent of the positive function of miR-127 in this pathway as described above. Then, we explored the potential links between miR-127 and these four genes. To do this, we constructed luciferase reporters containing wild-type 3′UTR of the four genes and performed dual-luciferase reporter assay. miR-127 did not affect the luciferase activity of *Fstl3*, *Smad7*, and *Ppm1b* 3′UTR constructs (Fig. 4*F*). However, miR-127 significantly decreased the luciferase activity of *Lefty2* 3′UTR construct. The specificity was confirmed by the reporter in which the binding site of miR-127 in the 3′UTR of *Lefty2* was mutant (Fig. 5*A*).

We then measured expression of *Lefty2* during EB differentiation and noted that it gradually decreased, and this was accompanied by increasing miR-127, in the process of EB differentiation (Fig. 5*B*). In addition, *Lefty2* was down-regulated in the miR-127-overexpressed ESCs at both RNA and protein levels compared with controls (Fig. 5, *C* and *D*). These data suggested that *Lefty2* is a novel target of miR-127.

Next, we assessed whether overexpression of *Lefty2* decreased the effect of miR-127 on mesendoderm differentiation. To do this, we co-transfected control oligonucleotides or miR-127 mimics and *Lefty2* overexpression vector into ESCs, and we examined the expression of specific markers on day 3 EBs. Compared with the cells transfected with miR-127 mimics, mesendoderm markers (*Foxa2* and *T*) were significantly decreased in the cells co-transfected with both miR-127 mimic and *Lefty2* overexpression vector (Fig. 5, *E* and *F*). A similar tendency of p-Smad2 was observed in these cells by Western blot (Fig. 5*F*). These data show that the overexpression of *Lefty2* could attenuate the role of miR-127 in promotion of mesendoderm differentiation. Taken together, our data suggested that miR-127 is involved in nodal signaling by down-regulating *Lefty2* to accelerate mesendoderm differentiation.

miR-127 Promotes Embryonic Shield Development in Zebrafish—In zebrafish, *lefty2* (*lft2*) possesses a conserved miR-127-targeting site. To investigate the function of miR-127 *in vivo*, we injected miR-127 mimics into one cell-stage embryos of zebrafish and analyzed the marker (*goosecoid* and *chordin*) expression of the embryonic shield area, which is the structure equivalent to the primitive streak in mice. Compared with the

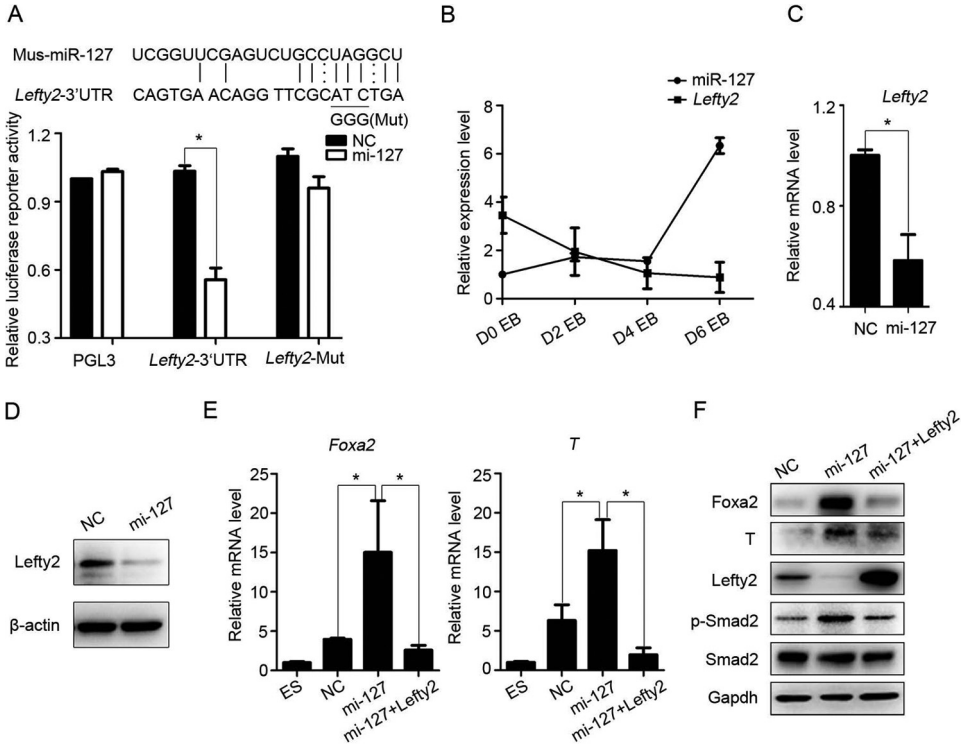

FIGURE 5. **miR-127 functions through nodal signaling by down-regulating *Lefty2*.** *A,* analysis of repression of *Lefty2* gene by miR-127 at the sequence of 3′UTR through a luciferase reporter assay. PGL3 vector acted as a control. These results from three independent experiments are shown as means ± S.E., *, $p < 0.05$. *B,* expression levels of miR-127 and *Lefty2*, measured by qRT-PCR during EB differentiation. Data are presented as means ± S.E. ($n = 3$). *C, Lefty2* expression analyzed by qRT-PCR in miR-127-overexpressed ESCs. The significance of expression was analyzed by Student's *t* test, and data are presented as means ± S.E. ($n = 3$, *, $p < 0.05$). *D,* Western blot showing Lefty2 expression in miR-127-overexpressed ESCs. β-Actin was used as loading control. *E,* qRT-PCR reveals expression of mesendoderm markers on day 3 EBs, transfected with random sequence, miR-127 mimic, or co-transfected with miR-127 mimic and *Lefty2* overexpressed vector, respectively. The significance of expression was analyzed by Student's *t* test, and data are presented as means ± S.E. ($n = 3$, *, $p < 0.05$). *F,* changes in expression of mesendoderm markers, p-Smad2 and Lefty2, are shown by Western blot, when miR-127 was overexpressed, or both miR-127 and *Lefty2* were overexpressed. Gapdh was used as loading control. *NC*, negative control.

non-injected embryos, the expression of *lft2*, examined by *in situ* hybridization, was dramatically down-regulated, although the expression of *chordin* and *goosecoid* (*gsc*) was obviously up-regulated in embryos injected with 20 μM miR-127 mimics at 6 h post-fertilization (Fig. 6*A*). The changed expressions of these genes were confirmed by qRT-PCR results (Fig. 6*B*). These results were consistent with the analysis of EB differentiation *in vitro*. In summary, we proposed a model in which miR-127 controls the mesendoderm differentiation via involvement in the nodal signaling pathway by regulating the expression of *Lefty2* (Fig. 7).

Discussion

miRNAs play important roles in multiple physiological and pathological processes (29–32). The mutations of key regulators of miRNA generation in mice, such as *Dicer* and *Dgcr8*, result in early embryonic lethality and defects of ESC differentiation, suggesting an important role of miRNAs in germ layer specification during mouse early embryonic development (15–18). In this study, we found the expression of miR-127 enriched in endoderm and PS of the E7.5 mouse embryo. Mouse EB differentiation assay showed that miR-127 overexpression led to elevated, but miR-127 knockdown decreased, mesendoderm marker expression. miR-127 knockdown also down-regulated expression of mesendoderm markers during the direct differentiation of mouse EpiSCs into mesendoderm. In addition, overexpression of miR-127 up-regulated the expression of embryonic shield markers in zebrafish embryos. All these results suggest that miR-127 possibly promotes PS development during mouse gastrulation.

Lefty2, an antagonist of activin/nodal signaling by competing to interact with the nodal receptor, plays an important role in PS formation and left-right axis patterning during mouse gastrulation (11, 33, 35). The *Lefty2* asymmetric expression pattern is regulated by SPC4 during mouse left-right axis formation (36). However, it is still not clear how *Lefty2* is regulated in mouse PS development. We found that miR-127 directly regulated *Lefty2* expression, as suggested by luciferase reporter assay. *Lefty2* is down-regulated in miR-127-overexpressed ESCs. The decreased expression of *Lefty2* is accompanied by increased expression of miR-127 during the differentiation of ESCs into EBs. Importantly, the effect of miR-127 on mesendoderm differentiation can be attenuated by overexpressed *Lefty2*. All of these results consistently suggest that miR-127 directly regulates the expression of *Lefty2* during mouse mesendoderm differentiation.

Although we found that miR-127 regulates mesendoderm differentiation, obvious developmental defects are not reported in miR-127 knock-out mice (20). miRNAs are regulators that fine-tune the expression of complementary mRNAs, and several miRNAs usually function together to regulate a given

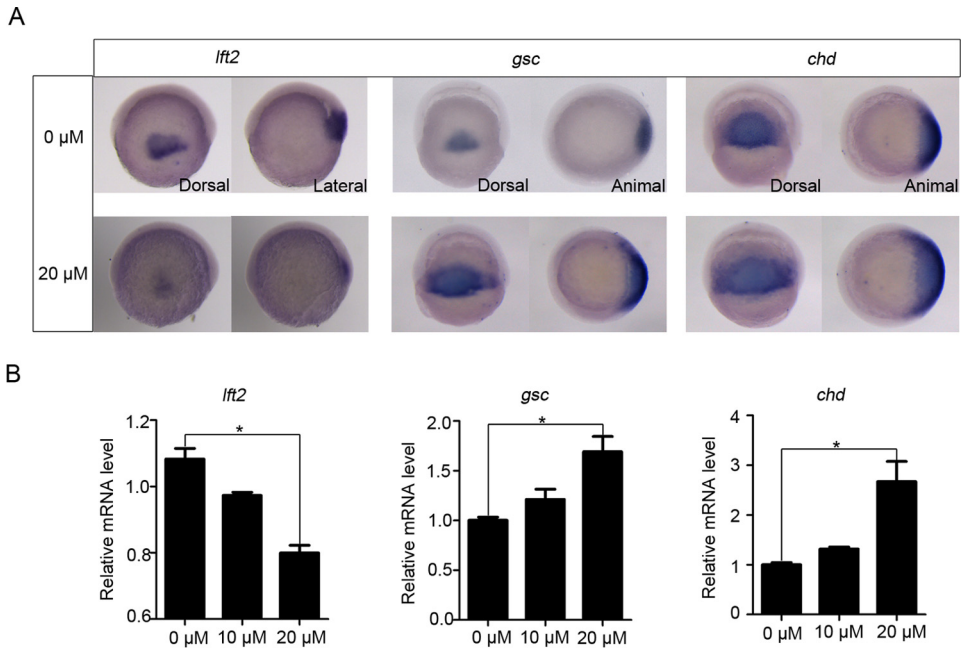

FIGURE 6. **miR-127 accelerates the development of zebrafish embryonic shield.** *A,* expression of embryonic shield markers and *Lefty2* measured with whole-mount *in situ* hybridization in miR-127 mimic-injected zebrafish embryos at concentrations of 0 and 20 μM. Embryos were injected with miR-127 mimics at the one-cell stage and harvested at 6 h post-fertilization for probing with indicated probes. *B,* qRT-PCR displaying embryonic shield markers and *Lefty2* expression in miR-127 mimic-injected zebrafish embryos, at concentrations of 0, 10, and 20 μM, respectively. The significance of expression was analyzed by Student's *t* test, and data are presented as means ± S.E. ($n = 3$, *, $p < 0.05$).

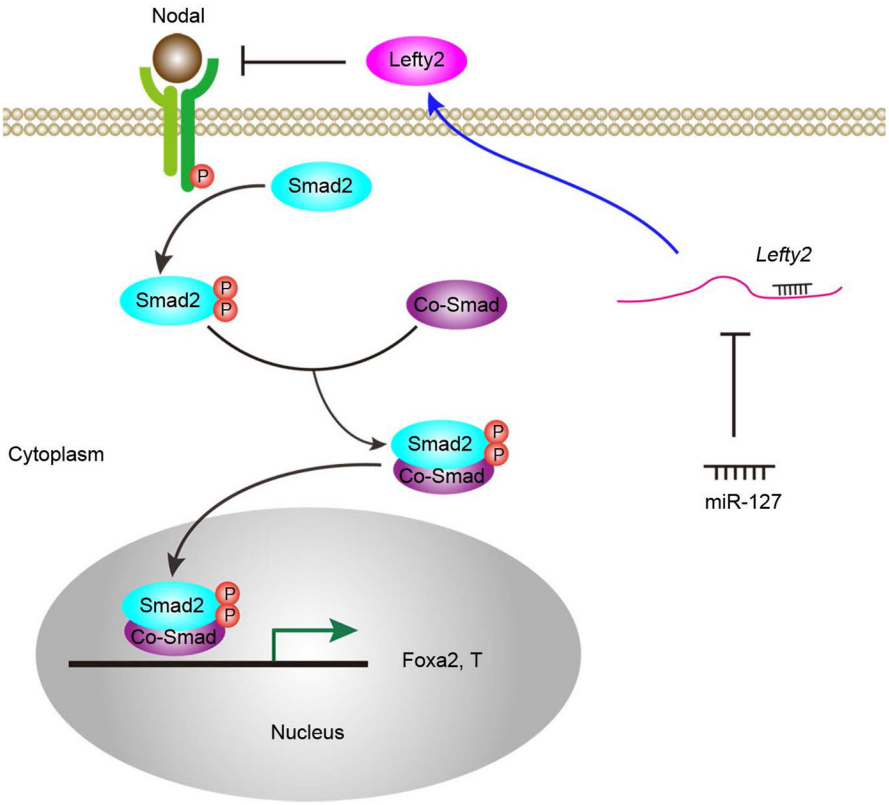

FIGURE 7. **Schematic representation depicts the mechanism of miR-127 in accelerating mesendoderm differentiation.** miR-127, through the complementary pairing, suppresses the expression of Lefty2, which is referred to as antagonist to the nodal pathway. Thus, miR-127 induces p-Smad2 expression and finally up-regulates expression of mesendoderm markers.

mRNA (37–39). Thus, other unknown factors may compensate the function of miR-127 in the knock-out mice. Mice with disruption to many important genes involved in differentiation are similar to miR-127 knock-out mice (22, 34, 40).

In summary, our data suggest that miR-127 is involved in mouse early embryonic development by controlling the expression of Lefty2, a critical regulator of PS formation. Our research reveals a novel function of miR-127 in accelerating mesendo-

derm differentiation and provides new evidence for the function of specific miRNAs in germ layer specification during gastrulation.

Author Contributions—H. M. designed and performed major experiments, analyzed the data, and wrote the manuscript. Y. L. conducted the experiments of zebrafish. Z.-A. Z. performed mouse embryo dissection and microarray. X. L. constructed Lefty2 overexpression vector. Y. Y. and X. Z. contributed to the results of EpiSCs. L. L. and Q. W. initiated and organized this project, analyzed the data, and wrote the manuscript. All authors commented on the manuscript.

References

1. Solnica-Krezel, L. (2005) Conserved patterns of cell movements during vertebrate gastrulation. *Curr. Biol.* **15,** R213–228
2. Tam, P. P., and Behringer, R. R. (1997) Mouse gastrulation: the formation of a mammalian body plan. *Mech. Dev.* **68,** 3–25
3. Heisenberg, C. P., and Solnica-Krezel, L. (2008) Back and forth between cell fate specification and movement during vertebrate gastrulation. *Curr. Opin. Genet. Dev.* **18,** 311–316
4. Conlon, F. L., Lyons, K. M., Takaesu, N., Barth, K. S., Kispert, A., Herrmann, B., and Robertson, E. J. (1994) A primary requirement for nodal in the formation and maintenance of the primitive streak in the mouse. *Development* **120,** 1919–1928
5. Schier, A. F., and Shen, M. M. (2000) Nodal signalling in vertebrate development. *Nature* **403,** 385–389
6. Schier, A. F. (2003) Nodal signaling in vertebrate development. *Annu. Rev. Cell Dev. Biol.* **19,** 589–621
7. Hoodless, P. A., Pye, M., Chazaud, C., Labbé, E., Attisano, L., Rossant, J., and Wrana, J. L. (2001) FoxH1 (Fast) functions to specify the anterior primitive streak in the mouse. *Genes Dev.* **15,** 1257–1271
8. Shen, M. M. (2007) Nodal signaling: developmental roles and regulation. *Development* **134,** 1023–1034
9. Hamada, H., Meno, C., Watanabe, D., and Saijoh, Y. (2002) Establishment of vertebrate left-right asymmetry. *Nat. Rev. Genet.* **3,** 103–113
10. Brennan, J., Lu, C. C., Norris, D. P., Rodriguez, T. A., Beddington, R. S., and Robertson, E. J. (2001) Nodal signalling in the epiblast patterns the early mouse embryo. *Nature*, 965–969
11. Meno, C., Gritsman, K., Ohishi, S., Ohfuji, Y., Heckscher, E., Mochida, K., Shimono, A., Kondoh, H., Talbot, W. S., Robertson, E. J., Schier, A. F., and Hamada, H. (1999) Mouse Lefty2 and zebrafish antivin are feedback inhibitors of nodal signaling during vertebrate gastrulation. *Mol. Cell* **4,** 287–298
12. Kim, V. N. (2005) MicroRNA biogenesis: coordinated cropping and dicing. *Nat. Rev. Mol. Cell Biol.* **6,** 376–385
13. Kim, V. N. (2005) Small RNAs: classification, biogenesis, and function. *Mol. Cells* **19,** 1–15
14. Han, J., Lee, Y., Yeom, K. H., Kim, Y. K., Jin, H., and Kim, V. N. (2004) The Drosha-DGCR8 complex in primary microRNA processing. *Genes Dev.* **18,** 3016–3027
15. Bernstein, E., Kim, S. Y., Carmell, M. A., Murchison, E. P., Alcorn, H., Li, M. Z., Mills, A. A., Elledge, S. J., Anderson, K. V., and Hannon, G. J. (2003) Dicer is essential for mouse development. *Nat. Genet.* **35,** 215–217
16. Murchison, E. P., Partridge, J. F., Tam, O. H., Cheloufi, S., and Hannon, G. J. (2005) Characterization of Dicer-deficient murine embryonic stem cells. *Proc. Natl. Acad. Sci. U.S.A.* **102,** 12135–12140
17. Kanellopoulou, C., Muljo, S. A., Kung, A. L., Ganesan, S., Drapkin, R., Jenuwein, T., Livingston, D. M., and Rajewsky, K. (2005) Dicer-deficient mouse embryonic stem cells are defective in differentiation and centromeric silencing. *Genes Dev.* **19,** 489–501
18. Wang, Y., Medvid, R., Melton, C., Jaenisch, R., and Blelloch, R. (2007) DGCR8 is essential for microRNA biogenesis and silencing of embryonic stem cell self-renewal. *Nat. Genet.* **39,** 380–385
19. Seitz, H., Youngson, N., Lin, S. P., Dalbert, S., Paulsen, M., Bachellerie, J. P., Ferguson-Smith, A. C., and Cavaillé, J. (2003) Imprinted microRNA genes transcribed antisense to a reciprocally imprinted retrotransposon-like gene. *Nat. Genet.* **34,** 261–262
20. Ito, M., Sferruzzi-Perri, A. N., Edwards, C. A., Adalsteinsson, B. T., Allen, S. E., Loo, T. H., Kitazawa, M., Kaneko-Ishino, T., Ishino, F., Stewart, C. L., and Ferguson-Smith, A. C. (2015) A trans-homologue interaction between reciprocally imprinted miR-127 and Rtl1 regulates placenta development. *Development* **142,** 2425–2430
21. Bhaskaran, M., Wang, Y., Zhang, H., Weng, T., Baviskar, P., Guo, Y., Gou, D., and Liu, L. (2009) MicroRNA-127 modulates fetal lung development. *Physiol. Genomics* **37,** 268–278
22. Zhao, Z. A., Yu, Y., Ma, H. X., Wang, X. X., Lu, X., Zhai, Y., Zhang, X., Wang, H., and Li, L. (2015) The roles of ERAS during cell lineage specification of mouse early embryonic development. *Open Biol.* **5,** 150092
23. Liu, Z., Lin, X., Cai, Z., Zhang, Z., Han, C., Jia, S., Meng, A., and Wang, Q. (2011) Global identification of SMAD2 target genes reveals a role for multiple co-regulatory factors in zebrafish early gastrulas. *J. Biol. Chem.* **286,** 28520–28532
24. Kattman, S. J., Witty, A. D., Gagliardi, M., Dubois, N. C., Niapour, M., Hotta, A., Ellis, J., and Keller, G. (2011) Stage-specific optimization of activin/nodal and BMP signaling promotes cardiac differentiation of mouse and human pluripotent stem cell lines. *Cell Stem Cell* **8,** 228–240
25. Tada, S., Era, T., Furusawa, C., Sakurai, H., Nishikawa, S., Kinoshita, M., Nakao, K., Chiba, T., and Nishikawa, S. (2005) Characterization of mesendoderm: a diverging point of the definitive endoderm and mesoderm in embryonic stem cell differentiation culture. *Development* **132,** 4363–4374
26. Mukherjee, A., Sidis, Y., Mahan, A., Raher, M. J., Xia, Y., Rosen, E. D., Bloch, K. D., Thomas, M. K., and Schneyer, A. L. (2007) FSTL3 deletion reveals roles for TGF-β family ligands in glucose and fat homeostasis in adults. *Proc. Natl. Acad. Sci. U.S.A.* **104,** 1348–1353
27. Hayashi, H., Abdollah, S., Qiu, Y., Cai, J., Xu, Y. Y., Grinnell, B. W., Richardson, M. A., Topper, J. N., Gimbrone, M. A., Jr., Wrana, J. L., and Falb, D. (1997) The MAD-related protein Smad7 associates with the TGFβ receptor and functions as an antagonist of TGFβ signaling. *Cell* **89,** 1165–1173
28. Lin, X., Duan, X., Liang, Y. Y., Su, Y., Wrighton, K. H., Long, J., Hu, M., Davis, C. M., Wang, J., Brunicardi, F. C., Shi, Y., Chen, Y. G., Meng, A., and Feng, X. H. (2006) PPM1A functions as a Smad phosphatase to terminate TGFβ signaling. *Cell* **125,** 915–928
29. Harfe, B. D. (2005) MicroRNAs in vertebrate development. *Curr. Opin. Genet. Dev.* **15,** 410–415
30. Bushati, N., and Cohen, S. M. (2007) MicroRNA functions. *Annu. Rev. Cell Dev. Biol.* **23,** 175–205
31. Colas, A. R., McKeithan, W. L., Cunningham, T. J., Bushway, P. J., Garmire, L. X., Duester, G., Subramaniam, S., and Mercola, M. (2012) Whole-genome microRNA screening identifies let-7 and mir-18 as regulators of germ layer formation during early embryogenesis. *Genes Dev.* **26,** 2567–2579
32. Wong, S. S., Ritner, C., Ramachandran, S., Aurigui, J., Pitt, C., Chandra, P., Ling, V. B., Yabut, O., and Bernstein, H. S. (2012) miR-125b promotes early germ layer specification through Lin28/let-7d and preferential differentiation of mesoderm in human embryonic stem cells. *PLoS ONE* **7,** e36121
33. Meno, C., Takeuchi, J., Sakuma, R., Koshiba-Takeuchi, K., Ohishi, S., Saijoh, Y., Miyazaki, J., ten Dijke, P., Ogura, T., and Hamada, H. (2001) Diffusion of nodal signaling activity in the absence of the feedback inhibitor Lefty2. *Dev. Cell* **1,** 127–138
34. Dawlaty, M. M., Ganz, K., Powell, B. E., Hu, Y. C., Markoulaki, S., Cheng, A. W., Gao, Q., Kim, J., Choi, S. W., Page, D. C., and Jaenisch, R. (2011) Tet1 is dispensable for maintaining pluripotency and its loss is compatible with embryonic and postnatal development. *Cell Stem Cell* **9,** 166–175
35. Meno, C., Saijoh, Y., Fujii, H., Ikeda, M., Yokoyama, T., Yokoyama, M., Toyoda, Y., and Hamada, H. (1996) Left-right asymmetric expression of the TGF β-family member lefty in mouse embryos. *Nature* **381,** 151–155
36. Constam, D. B., and Robertson, E. J. (2000) SPC4/PACE4 regulates a

TGFβ signaling network during axis formation. *Genes Dev.* **14,** 1146–1155
37. Sevignani, C., Calin, G. A., Siracusa, L. D., and Croce, C. M. (2006) Mammalian microRNAs: a small world for fine-tuning gene expression. *Mamm. Genome* **17,** 189–202
38. Yates, L. A., Norbury, C. J., and Gilbert, R. J. (2013) The long and short of microRNA. *Cell* **153,** 516–519
39. Ying, S. Y., and Lin, S. L. (2004) Intron-derived microRNAs–fine tuning of gene functions. *Gene* **342,** 25–28
40. Betschinger, J., Nichols, J., Dietmann, S., Corrin, P. D., Paddison, P. J., and Smith, A. (2013) Exit from pluripotency is gated by intracellular redistribution of the bHLH transcription factor Tfe3. *Cell* **153,** 335–347

MicroRNA-127 Promotes Mesendoderm Differentiation of Mouse Embryonic Stem Cells by Targeting Left-Right Determination Factor 2

Haixia Ma, Yu Lin, Zhen-Ao Zhao, Xukun Lu, Yang Yu, Xiaoxin Zhang, Qiang Wang and Lei Li

J. Biol. Chem. 2016, 291:12126-12135.
doi: 10.1074/jbc.M116.723247 originally published online April 12, 2016
